Translational Oncology 37 (2023) 101769

Contents lists available at ScienceDirect

Translational Oncology

journal homepage: www.elsevier.com/locate/tranon

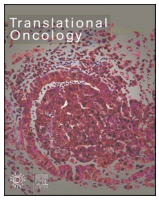

Original Research

Changes in leukoencephalopathy and serum neurofilament after (neo) adjuvant chemotherapy for breast cancer

Gwen Schroyen [a,b,c], Charlotte Sleurs [a,b,d,e], Tine Ottenbourgs [c], Nicolas Leenaerts [a,f,g,h], Ines Nevelsteen [b,e,i], Michelle Melis [a,b,c], Ann Smeets [b,e,i], Sabine Deprez [a,b,c,*], Stefan Sunaert [a,c,j]

[a] KU Leuven, Leuven Brain Institute, Leuven, Belgium
[b] University Hospitals Leuven, Leuven Cancer Institute, Leuven, Belgium
[c] KU Leuven, Department of Imaging and Pathology, Translational MRI, Leuven, Belgium
[d] Tilburg University, Department of Cognitive Neuropsychology, Tilburg, the Netherlands
[e] KU Leuven, Department of Oncology, Leuven, Belgium
[f] KU Leuven, Department of Neurosciences, Mind-Body Research, Leuven, Belgium
[g] KU Leuven, University Psychiatric Center, Leuven, Belgium
[h] University Hospitals Leuven, Department of Psychiatry, Leuven, Belgium
[i] University Hospitals Leuven, Department of Oncology, Surgical Oncology, Leuven, Belgium
[j] University Hospitals Leuven, Department of Radiology, Leuven, Belgium

ARTICLE INFO

Keywords:
Mri
Breast cancer
Chemotherapy
Leukoencephalopathy
Neurofilament

ABSTRACT

Background: Previous case studies have provided evidence for chemotherapy-induced leukoencephalopathy in patients with breast cancer. However, prospective research is lacking. Hence, we investigated leukoencephalopathy before and after chemotherapy and its association with a serum neuroaxonal damage marker.
Methods: This prospective cohort study included 40 patients receiving chemotherapy for breast cancer, and two age- and education-matched control groups, recruited between 2018 and 2021 (31–64 years of age). The latter control groups consisted of 39 chemotherapy-naïve patients and 40 healthy women. Fluid-attenuated inversion-recovery magnetic resonance imaging was used for lesion volumetry (total, juxtacortical, periventricular, infratentorial, and deep white matter) and blood serum to measure neurofilament light chain (NfL) levels. Acquisition took place pre-chemotherapy and three months and one-year post-chemotherapy, or at corresponding intervals. Within/between group differences were compared using robust mixed-effects modeling, and associations between total lesion volume and serum-NfL with linear regression.
Results: Stronger increases in deep white matter lesion volumes were observed shortly post-chemotherapy, compared with healthy women ($ß_{standardized}$=0.09, p_{FDR}<0.001). Increases in total lesion volume could mainly be attributed to enlargement of existing lesions (mean±SD, 0.12±0.16 mL), rather than development of new lesions (0.02±0.02 mL). A stronger increase in serum-NfL concentration was observed shortly post-chemotherapy compared with both control groups (β>0.70, p<0.004), neither of which showed any changes over time, whereas a decrease was observed compared with healthy women one-year post-chemotherapy (β=-0.54, p = 0.002). Serum-NfL concentrations were associated with lesion volume one-year post-chemotherapy (or at matched timepoint; β=0.36, p = 0.010), whereas baseline or short-term post-therapy levels or changes were not.
Conclusion: These results underscore the possibility of chemotherapy-induced leukoencephalopathy months post-treatment, as well as the added value of serum-NfL as a prognostic marker for peripheral/central neurotoxicity.
Translational relevance: Previous case studies have provided evidence of chemotherapy-induced leukoencephalopathy in patients with breast cancer. However, prospective studies to estimate longitudinal changes are currently missing. In this study, we used longitudinal fluid-attenuated inversion-recovery magnetic resonance imaging to assess white matter lesion volumes in patients treated for non-metastatic breast cancer and healthy women. Our findings demonstrate that chemotherapy-treated patients exhibit stronger increases in lesion volumes compared with healthy women, specifically in deep white matter, at three months post-chemotherapy.

* Corresponding author at: Radiology, UZ Leuven; UZ Herestraat 49 – box 7003; B-3000 Leuven, Belgium.
E-mail address: sabine.deprez@kuleuven.be (S. Deprez).

https://doi.org/10.1016/j.tranon.2023.101769
Received 31 March 2023; Received in revised form 21 August 2023; Accepted 21 August 2023

Increases could mainly be attributed to enlargement of existing lesions, rather than development of new lesions. Last, serum concentrations of neurofilament light chain, a neuroaxonal damage marker, increased shortly after chemotherapy and long-term post-chemotherapy levels were associated with lesion volumes. These findings highlight the potential of this non-invasive serum marker as a prognostic marker for peripheral and/or central neurotoxicity. Implementation in clinical practice could aid in therapeutic decisions, assessing disease activity, or monitoring treatment response.

Introduction

One in nine women will be confronted with breast cancer during her lifetime [1]. Most patients receive treatment with surgery, radiotherapy, endocrine therapy, targeted therapy and/or chemotherapy [2]. After treatment, unwanted side effects can occur, such as chronic fatigue or cognitive symptoms. Cancer-related cognitive impairment (CRCI) can occur in approximately 75% of women during [3] and up to 25% of women post-treatment [4]. However, because of its complexity, the underlying mechanisms of CRCI are insufficiently characterized [5].

Peripheral and central neurotoxicity have been observed with several chemotherapeutic agents [6]. Peripheral neurotoxicity may result from the direct action of these agents on the nervous system. By contrast, because most agents cannot cross the blood-brain barrier (e.g., cyclophosphamides, anthracyclines, taxanes), central neurotoxicity may result from metabolic alterations [6] produced indirectly by these agents.

Via fluid-attenuated inversion-recovery (FLAIR) magnetic resonance imaging (MRI), central neurotoxicity can be investigated non-invasively [7]. More specifically, pathological white matter (WM) can appear as hyperintense on these images because of increased water content [7]. Leukoencephalopathy for example, a term describing neurological disease affecting the WM, can appear soon after the initiation of high-dose chemotherapy for leukemia/lymphoma [8]. However, studies using FLAIR imaging in breast cancer patients are sparse, mainly showing negative findings when investigating WM lesion (WML) volumes [9,10] or neuroradiological ratings (e.g., Fazekas) [11]. These previous studies all applied cross-sectional designs. However, prospective evaluations of WML volumes could provide more insight into subtle changes that potentially contribute to CRCI.

In addition to neuroimaging, peripheral markers can provide information regarding neurotoxicity after cancer treatment. Although inflammatory markers (e.g., cytokines) have been widely investigated in breast cancer, evaluations of more direct neuronal integrity markers remain sparse [12]. With their exclusive expression in neurons, neurofilaments, such as neurofilament light chain (NfL), provide high prognostic and diagnostic accuracy for neuroaxonal damage in neurodegenerative disorders [13]. For breast cancer patients, we recently demonstrated 20-fold higher NfL-levels in chemotherapy-treated patients compared with healthy women or chemotherapy-naïve patients.

To investigate whether the neuroaxonal damage marker NfL could be useful as a potential precursor of observable damage to the WM, we assessed how WML volume changed from pre- to three months and one year post-chemotherapy in non-metastatic breast cancer patients, compared with chemotherapy-naïve patients or healthy women. Second, we investigated whether serum NfL levels changed over the same interval. Finally, we evaluated the association between WML volumes and serum NfL.

Materials and methods

Participants and study design

This prospective cohort study consecutively enrolled women aged ≤65 years from December 2018 to June 2021 at the University Hospitals Leuven (Fig. 1). Women diagnosed with non-metastatic breast cancer who were scheduled to receive (neo)adjuvant chemotherapy (C+; four

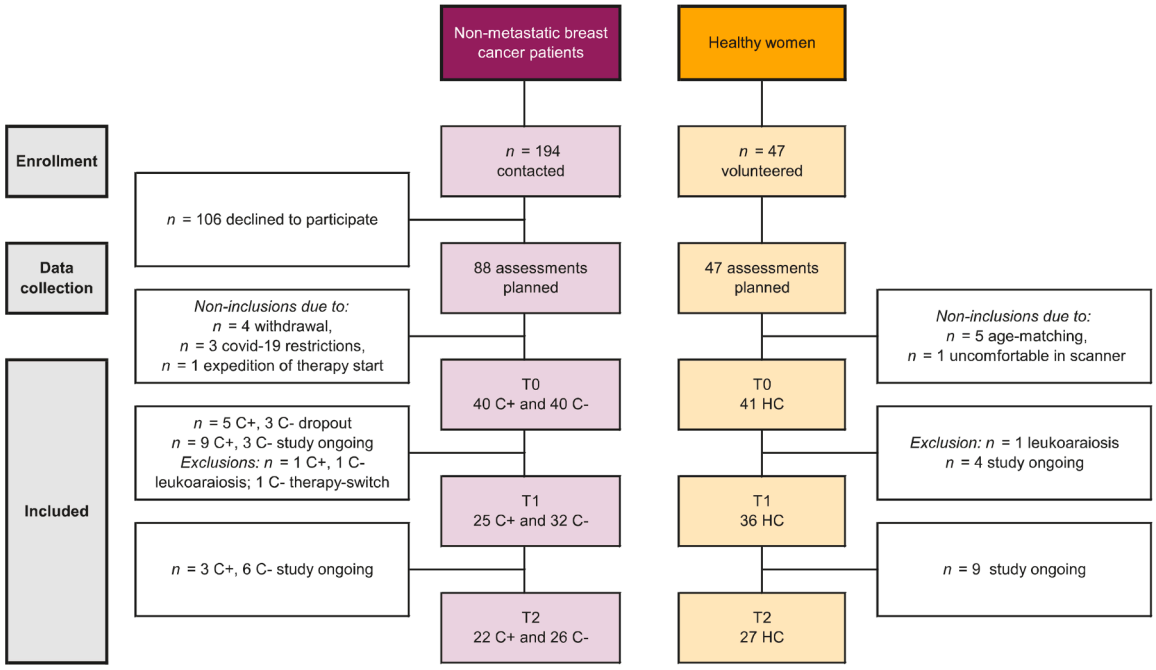

Fig. 1. Flow diagram of included participants. Abbreviations: C+ = patients scheduled to receive chemotherapy; C-, patients not scheduled to receive chemotherapy; HC, healthy controls. Note. Statistical analysis with mixed effects modeling ensured participants with incomplete time points could be included.

rounds of epirubicin 90 mg/m^2+cyclophosphamide 600 mg/m^2 and four to 12 rounds of paclitaxel 80 mg/m^2) and control patients who were not scheduled for chemotherapy (C-) were included. Eleven C+ patients (28%) received additional chemotherapy (carboplatine 80 mg/m^2 [n = 7] and/or capecitabine 1000 mg/m^2 [n = 4] or trastuzumab-emtansine 3.6 mg/kg [n = 2]). Patients underwent surgery, and some received additional radiotherapy and/or endocrine therapy (Table 1).

A second control group of healthy controls (HC) was recruited via response to online advertisements on the hospital's homepage. Both control groups, C- and HC, were matched at group level to the C+ group for age and education. Women with MRI contraindications, (history of) cancer treatment, drug or alcohol abuse, psychiatric/neurological condition/injury, intellectual disability, or systemic steroid use were excluded. Data collection for C+ patients was performed post-surgery or at diagnosis (T0), three months post-chemotherapy (T1, ~8 months after T0, interval including surgery/radiotherapy) and one year after ending chemotherapy (T2, ~9 months after T1). Controls were assessed at matched intervals, with T0 post-surgery for C- patients. Neuroimaging and blood sampling took place on the same day.

Table 1
Study population characteristics.

Characteristic	C+ n = 39		C- n = 39		HC n = 40	
	Mean with (95% CI) or n with (%)					
Age (years)	48	(45 - 51)	50	(48 – 52)	49	(46 – 51)
Education (years)	13	(12 - 14)	14	(13 – 15)	14	(14 – 15)
Verbal IQ (DART)	104	(95 - 112)	107	(101 – 113)	108	(105 – 111)
Body mass index (kg/m^2)	26	(24 - 27)	25	(23 – 26)	23	(22 – 24)
Postmenopausal at diagnosis	8	(21)	8	(21)	–	
Breast cancer stage: 0–1	12	(31)	38	(97)	–	
2	10	(26)	1	(3)	–	
3	17	(44)	0	(0)	–	
Cancer treatment: Neoadjuvant EC + T	21	(54)	–		–	
Adjuvant EC + T	18	(46)	–		–	
Adjuvant carboplatine	7	(18)	–		–	
Adjuvant capecitabine	4	(10)	–		–	
Adjuvant trastuzumab-emtansine	2	(5)	–		–	
Adjuvant targeted therapy	10	(26)				
Adjuvant radiotherapy	32	(82)	25	(64)	–	
Adjuvant aromatase inhibitor	21	(54)	13	(33)	–	
Adjuvant tamoxifen	0	(0)	15	(38)		
Adjuvant anti-HER2 therapy	5	(13)	–		–	
Neoadjuvant anti-HER2 therapy	7	(18)	–		–	
Days between T0 and T1	283	(251 – 316)	238	(228 – 248)	237	(227 – 247)
Days between T0 and T2	505	(494 – 516)	506	(501 – 511)	502	(496 – 509)

Abbreviations: BDI, Beck Depression Inventory; C+, breast cancer patients treated with chemotherapy; C-, chemotherapy-naïve patients with breast cancer; DART, Dutch Adult Reading Test; EC + T, epirubicin + cyclophosphamide and paclitaxel; FAS, fatigue assessment scale; HC, healthy controls; PSS, Perceived Stress Scale; STAI, Spielberger State-Trait Anxiety Inventory. Note. Years of education were counted starting from primary school. Dosing for chemotherapy: epirubicin 90 mg/m^2, cyclophosphamide 600 mg/m^2 and 4–12 rounds of paclitaxel 80 mg/m^2. A subset of patients (n = *11*) received additional carboplatine 80 mg/m^2 and/or capecitabine 1000 mg/m^2 or trastuzumab-emtansine 3.6 mg/kg. Targeted therapy consisted of pembrolizumab (study related), pertuzumab, trastuzumab or ribociclib (study related). The breast cancer stage was defined according to Hortobagyi et al. [14].

Magnetic resonance neuroimaging

All participants underwent a one-hour whole-brain MRI scanning-protocol (3T Philips Achieva, 32-channel phased-array head-coil). After a ~6-minute high-resolution T1-weighted image (MPRAGE; 208 sagittal slices, voxel=0.80 mm isotropic, TR/TE=5.8/2.5 ms, FA=8°, FOV=320 × 320 × 208), a ~5-minute FLAIR scan was acquired (183 sagittal slices, voxel=1 mm isotropic, TR/TE=4800/340 ms, FA=40°, FOV=256 × 256, NSA=2). Additional sequences were acquired beyond the scope of this manuscript. FLAIR data were excluded (n = 3 HC) because of corrupt data (n = 2 T0) or motion artefacts (n = 1 T2).

FLAIR WM hyperintensity quantification

Brain tissue (gray matter, WM) and lesion volumes (mL) were quantified based on T1 and FLAIR images using the icometrix icobrain ms software [15,16]. This approach has been validated on large multi-scanner, multi-center datasets, and it was Food and Drug Administration and CE approved. It combines an unsupervised method with a supervised deep-learning method. In the unsupervised part, an expectation maximization algorithm optimizes a Gaussian mixture model on the image intensities while correcting for field inhomogeneities, guided by probabilistic tissue priors. The algorithm includes a spatial consistency model based on a Markov random field and iterates between the FLAIR lesion segmentation and tissue class segmentation of the lesion-filled T1-weighted image until convergence. The lesion segmentations were refined using a deep-learning attention-gate 3D U-net network. This deep-learning network was specifically trained to improve the segmentation of infratentorial and juxtacortical plaques. Thus, total lesion volumes were quantified across the whole brain and per anatomical region [16] according to the McDonald criteria [17] (i.e. periventricular, infratentorial, juxtacortical or deep white matter). In the second step, the software evaluates longitudinal changes by performing a joint segmentation algorithm of the lesions of two subsequent scans while explicitly quantifying new lesions and growing lesions. The longitudinal icobrain pipeline is evaluated on pairs of consecutive time points to compute the percentage volume change in lesions [15]. For patients with more than two time points, the volumes per time point were computed by cumulating the volume changes that result from pairwise longitudinal analyses.

Serum measurement

Blood samples were centrifuged, and supernatant stored at −80 °C. NfL was assessed with an enzyme-linked immunosorbent kit (Uman-Diagnostics, Umea) on serum [18] and quantified with an electrochemiluminescent assay [19]. The distribution of groups was equal across plates, and the mean values across triplicates (separate plate assays) were used for analysis. The coefficient of variation (standard deviation/mean) was calculated; mean intraplate variability was 11% and mean interplate variability 45%. Samples below the detection limit were converted to their corresponding limits. Triplicate values of one HC (T0) were below the detection limit and outcomes subsequently excluded.

Statistical analysis

Statistical analyses were performed using Rv4.1.2. Data were transformed (natural log transformation with base e) if they showed a non-Gaussian distribution. Between- and within-group differences in changes of WML volume and NfL were estimated with robust linear mixed-effects models using the DAStau-method (robustlmm-package, version 2.4–5). In this way, we were able to provide estimates where outliers or other contamination have little influence (robust) as well as account for (unbalanced) repeated measures and missingness in the data (mixed effects), still making use of subjects containing single time-point

data [20,21]. Models included WML or NfL as dependent variable, a random subject intercept to account for repeated measures, and time, group, and an interaction between time and group as fixed effects, correcting for age. Benjamini-Hochberg (false discovery rate, FDR) correction was used to compare multiple (here: four) lesion volume outcomes. Second, explorative linear regression models were constructed to evaluate the association between outcomes (i.e., NfL levels and WML volume). Specifically, associations between both the NfL levels for each timepoint, as well as changes in NfL from T0 to T1, and WML were assessed, correcting for age. Because of the cumulative nature of WML burden throughout time, only lesion volumes at T2 and changes from T0 to T2 were used for these associations. Continuous variables were standardized for model interpretation; estimates can therefore be interpreted as effect sizes. Statistical significance was set at $p_{(FDR)}<0.05$.

Results

Participants

Of the 194 eligible patients, 88 provided informed consent, for whom assessments were planned (Fig. 1). Of those, eight participants were not included (four withdrew, three could not be rescheduled due to covid-19 restrictions and one patient's treatment start was expedited). Forty-seven HCs volunteered to participate, of which six were excluded (one withdrew, five age-matched). A total of 121 women participated in this study: 40 C+ patients (mean±SD, 48±9 years), 40 C- patients (50±7 years) and 41 HCs (49±9 years). Three participants were excluded because of extreme leukoaraiosis on MRI (one C+, one C-, one HC). Additionally, because of covid-19 restrictions, a T1 assessment of one C+ patient and a T2 assessment of one C- patient were scheduled >3 interquartile ranges later than the median interval times and were excluded. BMI was higher in C+ patients than in HC, but not in C- patients. The results presented here constitute data collected until December 2021; data collection for T1 and T2 is ongoing. Subject demographics and medical information are summarized in Table 1.

FLAIR WM hyperintensities

Table 2 and Fig. 2 present the FLAIR WM hyperintense lesion volumes of all participants.

At baseline, no group differences in lesion volumes were observed (Fig. 2A). In C+ patients, increased lesion volumes were observed shortly post-chemotherapy, in the deep WM (from T0 to T1; standardized ß and 95% confidence interval (CI)=0.07 (0.03, 0.11), p_{FDR}=0.002). These effects were not found for total WM lesion volume, nor in the periventricular or juxtacortical WM. This increase in deep WM volume was also stronger for C+ patients compared with the HC group (β=0.09 (0.04, 0.14), $p_{FDR}<0.001$), but not compared to C- patients. No differences in evolution of lesion volumes from T0 to T2 within or between groups were observed. Age was significantly associated with total, deep, and periventricular WM lesion volume, across groups and timepoints ($\beta>0.29$ (0.10, 0.42), $p_{FDR}<0.002$).

The longitudinal icobrain analysis (Fig. 2B) revealed that enlargement of lesions mainly occurred, whereas newly formed lesions were limited. More specifically, C+ patients showed a stable enlargement of mean 0.12 mL at both time points, whereas a stable 0.08 mL (C- patients) and 0.06 and 0.10 mL (HCs) enlargement was observed for controls at T1 and T2, respectively. By contrast, newly formed lesions were <0.04 mL for all groups.

Serum NfL

At baseline, C+ patients presented with significantly higher serum levels of NfL than HCs (T0: standardized ß with 95% CI=0.50 (0.10, 0.90), $p = 0.002$), but not C- patients (Fig. 3A). For C+ patients, NfL

Table 2
FLAIR WM hyperintensity volumes and serum NfL concentrations.

Characteristic	C+ *T0: n = 39 T1: n = 25 T2: n = 22*		C- *T0: n = 39 T1: n = 32 T2: n = 26*		HC *T0: n = 40 T1: n = 36 T2: n = 27*	
	Mean with (SD; range)					
total brain tissue volume at t0 (ml):						
Gray matter	920	(41; 867 - 1027)	911	(35; 843 - 977)	924	(43; 841 - 995)
White matter	631	(25; 591 - 676)	623	(26; 563 - 697)	620	(24; 571 - 666)
FLAIR WM hyperintensity (mL):						
Total T0	1.65	(1.8; 0.27 - 7.81)	1.65	(1.0; 0.58 - 4.70)	1.60	(0.9; 0.27 - 3.93)
Total T1	1.87	(2.1; 0.27 - 7.91)	1.85	(1.2; 0.00 - 4.74)	1.51	(1.0; 0.28 - 3.88)
Total T2	2.10	(2.4; 0.38 - 8.19)	1.78	(1.1; 0.56 - 4.82)	1.62	(1.0; 0.37 - 4.06)
Periventricular T0	1.13	(1.0; 0.26 - 4.88)	1.34	(0.7; 0.32 - 3.59)	1.27	(0.8; 0.16 - 3.49)
Periventricular T1	1.22	(1.3; 0.22 - 5.13)	1.34	(0.8; 0 - 3.64)	1.18	(0.8; 0.18 - 3.47)
Periventricular T2	1.35	(1.4; 0.28 - 6.64)	1.30	(0.8; 0.32 - 3.72)	1.29	(0.9; 0.24 - 3.62)
Deep white matter T0	0.42	(0.9; 0 - 4.63)	0.40	(0.4; 0 - 1.38)	0.26	(0.2; 0 - 1.03)
Deep white matter T1	0.54	(1.1; 0 - 4.81)	0.41	(0.4; 0 - 1.42)	0.25	(0.2; 0 - 1.12)
Deep white matter T2	0.63	(1.2; 0.01 - 4.98)	0.39	(0.4; 0.03 - 1.39)	0.23	(0.3; 0 - 1.21)
Juxtacortical T0	0.08	(0.1; 0 - 0.49)	0.07	(0.1; 0 - 0.36)	0.06	(0.1; 0 - 0.53)
Juxtacortical T1	0.10	(0.1; 0 - 0.50)	0.07	(0.1; 0 - 0.38)	0.06	(0.1; 0 - 0.50)
Juxtacortical T2	0.11	(0.1; 0 - 0.49)	0.07	(0.1; 0 - 0.36)	0.07	(0.1; 0 - 0.49)
Total new at T1 vs. T0	0.02	(0.02; 0 - 0.06)	0.02	(0.02; 0 - 0.07)	0.01	(1; 0 - 0.04)
Total new at T2 vs. T1	0.02	(0.02; 0 - 0.11)	0.02	(0.02; 0 - 0.06)	0.04	(0.09; 0 - 0.48)
Total enlarging at T1 vs. T0	0.12	(0.16; 0.01 - 0.53)	0.08	(0.10; 0 - 0.46)	0.06	(0.05; 0 - 0.23)
Total enlarging at T2 vs. T1	0.12	(0.21; 0 - 0.94)	0.08	(0.09; 0 - 0.33)	0.10	(0.08; 0 - 0.32)
Serum NfL concentration (pg/mL):						
T0	15.20	(18; 5.82 - 67.63)	14.53	(17; 1.85 - 69.88)	12.58	(11; 3.76 - 48.45)
T1	39.25	(40; 4.62 - 161.32)	14.13	(9; 3.06 - 37.75)	11.80	(16; 4.63 - 63.54)
T2	15.75	(10; 5.31 - 43.20)	12.59	(12; 7.15 - 65.31)	14.77	(15; 2.18 - 77.82)

Abbreviations: C+, breast cancer patients treated with chemotherapy; C-, chemotherapy-naïve patients with breast cancer; FLAIR, fluid-attenuated inversion recovery scan; HC, healthy controls; NfL, neurofilament-light chain;

T0, time point before chemotherapy; T1, time point after surgery + chemotherapy + radiotherapy; T2, time point one year after ending chemotherapy for C+ patients; and at matched interval timepoints for HC and C- patients; WM, white matter.

increased shortly post-chemotherapy (from T0 to T1: β=0.70 (0.37, 1.02), p<0.001) and decreased one-year post-chemotherapy (from T0 to T2: β=−0.54 (−0.89, −0.20), p = 0.002) compared with pre-chemotherapy. No changes over time were observed for C- patients or HCs. A stronger short-term increase in concentration was observed for C+ patients than for C- patients (T0 to T1: β=0.82 (0.38, 1.26), p<0.001) and HCs (β=0.66 (0.22, 1.10), p = 0.004). A stronger long-term decrease was observed for C+ patients compared with the stable levels in the HC group (T0 to T2: β=−0.63 (−1.10, 0.16), p = 0.009), but not when compared with C- patients.

Associations of WM hyperintensities and serum NfL

The associations of NfL concentration (at T0, T1 and T2 as well as the short-term changes [change score from T0 to T1]) with WML volume (at T2 and long-term changes [change score from T0 to T2]) were evaluated for complete cases (n = 19 C+, 25 C- and 26 HC). Serum NfL concentration at T2 was associated with total WML volume at T2 (standardized ß and 95% CI=0.36 (0.09, 0.62), p = 0.010, Fig. 3B), with age also contributing significantly as covariate (β=0.43 (0.21, 0.66), p<0.001). NfL concentrations measured at T0 or T1 did not precede WML at T2. Moreover, short-term changes in NfL were not associated with lesion volume at T2, nor with long-term changes in lesion volumes (Fig. 3C). Post hoc associations at T0 or T1 of NfL with WML volume, both at the same time-point, also showed no associations (data not shown).

Discussion

The present study explored the occurrence of white matter lesions during the course of breast cancer treatment and its possible association with a serum marker for neuroaxonal damage. Shortly after chemotherapy, a stronger increase in lesion volume was observed in the deep WM of patients with breast cancer, even after adjustment for age. In contrast, periventricular lesion volumes were mainly influenced by age, with no additional cancer or treatment effects. Notably, juxtacortical

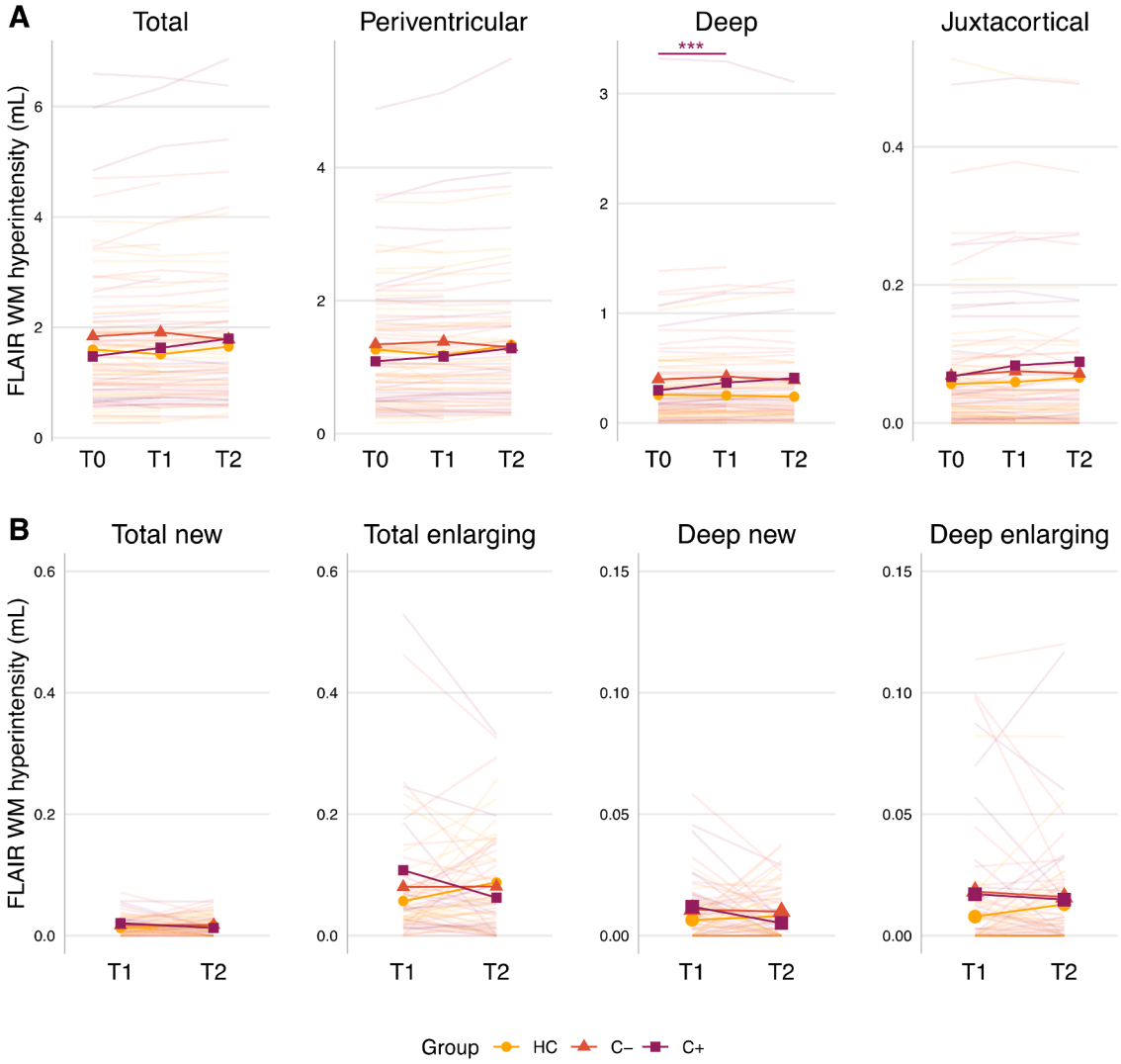

Fig. 2. Short- and long-term changes in white matter lesion volumes. Individual and mean line plots per group are presented. A) Robust linear mixed effects models, corrected for age, showed a transient increase in deep white matter lesion volume (for n = 274 observations from 114 participants). B) Longitudinal analysis of FLAIR images showed increased lesion volumes were mainly due to enlargement of existing lesions, rather than development of new ones. Abbreviations: C+, breast cancer patients treated with chemotherapy; C-, chemotherapy-naïve breast cancer patients; FLAIR, fluid-attenuated inversion recovery scan; HC, healthy controls; T0, time point before chemotherapy; T1, time point after surgery + chemotherapy + radiotherapy; T2, time point one year after ending chemotherapy for C+ patients; and at matched interval timepoints for HC and C- patients; WM = white matter. p_{FDR}<0.01**, <0.001***, full purple line = C+ significant time effects.

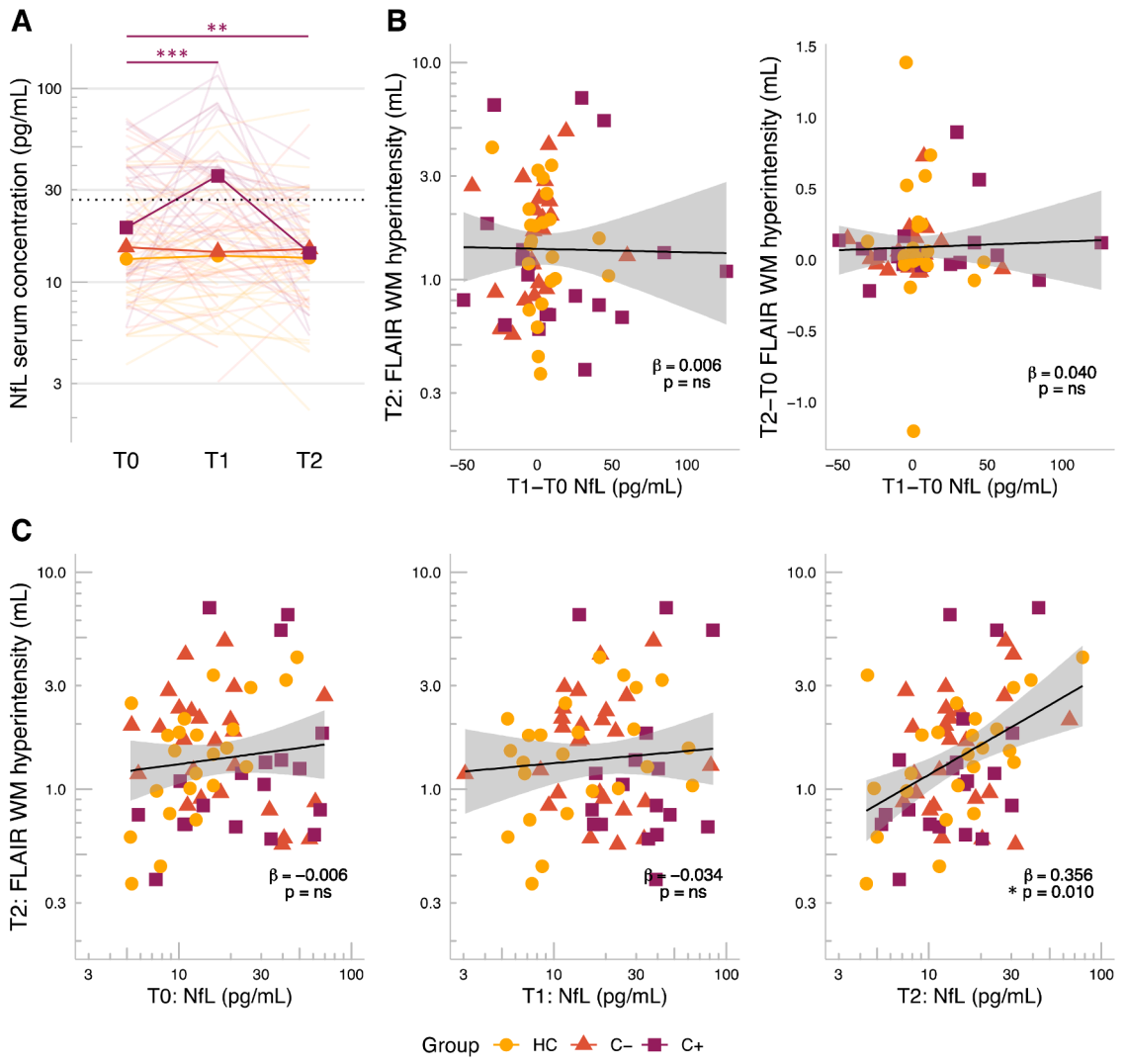

Fig. 3. Short- and long-term changes in serum NfL and its linear relationship with white matter lesion volumes. A) Robust linear mixed effects models, corrected for age, showed a transient increase in serum NfL concentration after chemotherapy (for $n = 206$ observations from 106 participants), decreasing to lower concentrations than baseline levels. Dotted line = cut-off for neurodegenerative disease, proposed by Gaiottino et al. [19]. B-C) General linear regression models, corrected for age, showed (for $n = 71$ participants). B) Lesion volume at T2 was associated with serum NfL at T2, but not T0 or T1; and C) lesion volume at T2 or change in lesion volume from T0 to T2 was not associated with change in NfL from T0 to T1. Lines represent linear regression models with shaded 95% confidence intervals. Abbreviations: C+, breast cancer patients treated with chemotherapy, C-, chemotherapy-naïve breast cancer patients; FLAIR = fluid-attenuated inversion recovery scan; HC, healthy controls; ns = non-significant, NfL, neurofilament-light chain; T0, time point before chemotherapy; T1, time point after surgery + chemotherapy + radiotherapy; T2, time point one year after ending chemotherapy for C+ patients; and at matched interval timepoints for HC and C- patients. $p<0.05$*, <0.01**, <0.001***, full purple line = C+ significant time effects.

lesion volumes did not show any associations with either age or cancer treatment. Additionally, NfL clearly coincided with the treatment trajectory of chemotherapy, peaking one month post-treatment (for example, because of peripheral neurotoxicity) and returning to normal levels one year post-chemotherapy. Absolute levels of NfL were associated with lesion volumes one year after chemotherapy (or matched timepoint). In contrast, baseline, post-chemotherapy, or acute changes in NfL levels were not associated with WML or changes in volume. Taken together, our results underscore the potential of NfL as a prognostic marker for the occurrence of subtle leukoencephalopathy, especially after administration of chemotherapeutic agents.

Increase in WM lesion volume

Previous limited evidence exists based on case studies for the presence of chemotherapy-induced leukoencephalopathy, measured as WM hyperintensities [22–24]. For example, a woman who completed chemotherapy that was comparable to the treatment in the current study (doxorubicin, cyclophosphamide, and docetaxel) presented with higher WML volumes than her healthy, chemotherapy-naïve, monozygotic twin (9.8 versus 6.2 mL) [24]. By contrast, more recent cross-sectional studies did not observe difference between breast cancer patients and healthy controls from one month [25], six months [26], ten years [11] or 20 years post-chemotherapy [27]. In the current study, we present the first prospective evidence for increased WML post-chemotherapy, more specifically in the deep WM.

The existing hypotheses on the underlying pathology of such WM lesions is non-specific and includes multiple mechanisms. Chemotherapeutic drugs might induce changes in neuronal/glial cell plasticity and survival, via disturbance of myelin/glucose synthesis, increased cytokine concentration, and oxidative stress, as observed in rodents [6]. For instance, persistent microglial activation can induce disrupted/dysregulated myelination, eventually resulting in axonal damage [28,29]. In our previous work, we observed increased

neuroinflammation in juxtacortical lesions when compared to normal-appearing WM [25], suggesting inflammatory pathways concurring with WM pathology (possibly with underlying demyelination). In the current study, deep, rather than juxtacortical WM lesion volumes increased. This suggests other pathophysiological mechanisms to be involved besides acute inflammatory mechanisms. Although mechanisms could be different across the applied chemotherapy agents, we were unable to differentiate between their potential toxicity or dosages because only a subset of participants ($n = 11$) received additional chemotherapy beyond the inclusion therapy paradigm. However, based on existing case reports, cyclophosphamide is most associated with encephalopathy, suggested mainly because of oxidative damage [6], potentially also inducing central toxicity here.

Besides induced toxicity, our findings could also be age-related, because increasing age and decline in cardiovascular health are known risk factors for clinically silent brain injuries, such as WML [30] in, for example, periventricular regions [31]. Nevertheless, considering the absence of changes in lesion volumes among the control groups, there is still suggestive evidence of an additional (combination) effect resulting from cancer and its treatment. Although lesions appeared to increase post-chemotherapy, this phenomenon could also be caused by long-term effects of more advanced disease stage because this intrinsically differs between patients being scheduled to receive chemotherapy or not (e.g., tumor grade, ER/PR/HER2 receptor status). Combined, our results underscore the hypothesis of chemotherapy- or advanced disease state-induced localized lesions presenting different entities, with deep WM lesions possibly being more sensitive to such toxicity. Furthermore, development of other lesions (i.e., periventricular) could be more age-related, and short-term neuroinflammation might not necessarily precede the more superior (i.e., juxtacortical) lesion development. Future studies are necessary to elaborate on the potential differences in pathophysiology of localized WM lesions.

Serum NfL associating with central toxicity

In this study, serum NfL concentrations were higher three months post-chemotherapy (median=39 pg/mL), compared with baseline, but did not reach the peak level that was observed previously, at only one month post-chemotherapy (median=339 pg/mL) [32]. Furthermore, NfL values stabilized to levels observed in healthy women at the later timepoint (median=15 pg/mL). In other words, the serum NfL concentration appeared to match with the treatment trajectory because it increased shortly after chemotherapy and decreased with the wash-out of chemotherapeutic agents. This hypothesis is supported by a NfL half-life of months [33] and previous studies that have shown chemotherapy dose-dependent increases in NfL levels in patients with breast cancer [34,35].

Increases in NfL could reflect both central nervous system or peripheral neuroaxonal injury [13]. Next, we provide possible origins of these increased NfL levels. First, tumor biology (or l disease stage in general) could have influenced NfL concentration. At baseline, a higher level of NfL was observed in chemotherapy-treated patients (and too a smaller extent in control patients). It is possible that more aggressive tumors may impact the tumoral microenvironment, blood vessels, and nervous system at a microstructure level, leading to elevated NfL levels. However, because lower values are more susceptible to measurement errors, this could have introduced a bias. Our results underscore the need for (more sensitive; e.g., SIMOA assay [13]) investigations disentangling baseline characteristics from treatment effects. Second, treatment-induced damage to peripheral nerves could increase serum NfL. In this context, an invasive procedure such as brain surgery was shown to elevate NfL, levels shortly post-surgery [36]. In the same way, breast cancer surgery could have accounted for *higher baseline* levels of NfL. Additionally, *peripheral* neuropathy, a well-known side effect of chemotherapy [37] (and radiotherapy [38]), is also associated with NfL increases in breast cancer [35,39] and other non-cancer [40,41] populations. Therefore, increased serum NfL levels could reflect peripheral axonal abnormalities, which was potentially induced by paclitaxel treatment [39]. Third, treatment-induced central neurotoxicity could also underlie increased NfL levels. Indeed, in patients with multiple sclerosis, NfL appears as an initial precursor of lesions, as well as showing concurrent associations [42]. In the presented oncological population, we observed that changes in NfL did not precede WML, but *absolute* levels measured one year after chemotherapy were associated with lesion volumes at the same timepoint. These results underscore NfL as a potential marker of central long-term neurotoxicity. When investigating WM microstructural changes with diffusion-weighted parameters, abundant research has confirmed chemotherapy-associated changes in normal-appearing WM [32,43,44]. Moreover, we previously observed that serum NfL, measured shortly post-chemotherapy for breast cancer, was associated with brain patterns of neuroinflammation [32]. The observed association between NfL and late lesion volumes could consequently suggest that the earlier observed WM microstructural changes represent neuroaxonal damage, rather than sole damage to the myelin, which is potentially influenced by neuroinflammation. Future multi-dimensional research (e.g., combining myelin-water and diffusion imaging with NfL and inflammatory markers) could differentiate between such microstructural changes, which FLAIR imaging cannot. In parallel, better characterization of the neurobiological mechanisms of serum neurofilament is required [45].

Limitations and future perspectives

Since multi-agent chemotherapy was administered, translation from preclinical studies will be necessary to differentiate agents most involved in toxicity. Second, although we controlled for age in our models, other factors, such as dietary deficiencies, genetic predispositions, and renal impairment, can additionally increase the probability of neurotoxicity [6]. Third, the interval between T0 and T1 was greater for C+ patients than for both control groups, given that 11 patients needed to receive additional chemotherapy and most patients were scheduled for additional endocrine therapy and/or radiotherapy. These factors could potentially have influenced the results. However, by including a chemotherapy-naïve control group, we could partly control for these potential treatment effects.

Because clinical thresholds have been defined for serum NfL estimating peripheral neuropathy [35], thresholds for induced cerebral pathophysiology could further be identified. Whilst previous neuroimaging studies have shown associations between microstructural changes and cognitive decline after cancer [12], these changes are mostly subtle and neuroimaging remains cumbersome and expensive. Consequently, measurement of serum neurofilaments can further be explored as an add-on or more easily accessible alternative to neuroimaging for cognitive decline or cerebral damage. Moreover, although the existing evidence remains limited, serial serum NfL is suggested to be as sensitive as MRI for treatment evaluation in multiple sclerosis patients [46]. Interestingly, one recent study explored the potential of serum NfL as a biomarker for subjective cognitive complaints after paclitaxel treatment for breast cancer [47]. Whilst they did not observe any association in their sample of 20 patients, further evaluation in larger samples and other treatments is warranted. In parallel, the predictive value of serum NfL for long-term central versus peripheral neurotoxicity should be investigated further. In conclusion, serial measurements of NfL throughout cancer treatments could have a clinical impact as a potential marker to support therapeutic decisions, monitoring disease activity, or treatment response [45].

Conclusion

This was the first prospective study to evaluate changes in neuroaxonal damage by assessing NfL and leukoencephalopathy, in patients treated for non-metastatic breast cancer. We showed a stronger short-

term increase in deep WM lesion volume and serum NfL after chemotherapy, both stabilizing one year post-chemotherapy. Moreover, if levels of NfL persisted to be high, they associated with larger lesion volumes one year post-chemotherapy, aiding the use of this neuroaxonal damage marker to identify the presence of central neurotoxicity. Future studies evaluating the association between serum NfL, lesion load, and cognitive impairment will be critical in elucidating underlying biology of neurocognitive impairments after cancer therapy.

Declarations

This study was approved by the local Ethic Committee Research UZ / KU Leuven (February 2018, S60515) and was conducted in accordance with the Declaration of Helsinki. All participants provided written informed consent.

Funding

GS is supported by Research Fund KU Leuven (C24/18/067) and Stichting tegen Kanker. NL is supported by Research Fund KU Leuven (C14/18/096). MM is supported by Research Foundation Flanders (1S68621N). Funding sources provided financial contributions.

CRediT authorship contribution statement

Gwen Schroyen: Conceptualization, Data curation, Formal analysis, Funding acquisition, Investigation, Methodology, Project administration, Software, Visualization, Writing – original draft, Writing – review & editing. **Charlotte Sleurs:** Conceptualization, Methodology, Resources, Software, Validation, Writing – original draft, Writing – review & editing. **Tine Ottenbourgs:** Data curation, Investigation, Project administration, Writing – review & editing. **Nicolas Leenaerts:** Methodology, Software, Writing – review & editing. **Ines Nevelsteen:** Resources, Validation, Writing – review & editing. **Michelle Melis:** Investigation, Project administration, Writing – review & editing. **Ann Smeets:** Resources, Supervision, Validation, Writing – review & editing. **Sabine Deprez:** Conceptualization, Funding acquisition, Methodology, Resources, Supervision, Validation, Visualization, Writing – review & editing. **Stefan Sunaert:** Conceptualization, Data curation, Formal analysis, Methodology, Resources, Software, Supervision, Validation, Writing – review & editing.

Declaration of Competing Interest

The authors have no conflict to declare.

Data availability

The data generated in this study are available upon reasonable request from the corresponding author.

References

[1] H. Sung, J. Ferlay, R.L. Siegel, et al., Global cancer statistics 2020: GLOBOCAN estimates of incidence and mortality worldwide for 36 cancers in 185 countries, CA Cancer J. Clin. 71 (3) (2021) 209–249, https://doi.org/10.3322/caac.21660.
[2] F. Cardoso, S. Kyriakides, S. Ohno, et al., Early breast cancer: ESMO clinical practice guidelines for diagnosis, treatment and follow-up, Ann. Oncol. 30 (8) (2019) 1194–1220, https://doi.org/10.1093/ANNONC/MDZ173.
[3] M.C. Janelsins, S.R. Kesler, T.A. Ahles, G.R. Morrow, Prevalence, mechanisms, and management of cancer-related cognitive impairment, Int. Rev. Psychiatry 26 (1) (2014) 102–113, https://doi.org/10.3109/09540261.2013.864260.
[4] A.B.C. Dijkshoorn, H.E. van Stralen, M. Sloots, S.B. Schagen, J.M.A. Visser-Meily, V.P.M. Schepers, Prevalence of cognitive impairment and change in patients with breast cancer: a systematic review of longitudinal studies, Psychooncology (2021), https://doi.org/10.1002/pon.5623.
[5] T.A. Ahles, J.C. Root, Cognitive effects of cancer and cancer treatments, Annu. Rev. Clin. Psychol. 14 (1) (2018) 425–451, https://doi.org/10.1146/annurev-clinpsy-050817.
[6] C. Pellacani, G. Eleftheriou, Neurotoxicity of antineoplastic drugs: mechanisms, susceptibility, and neuroprotective strategies, Adv. Med. Sci. 65 (2) (2020) 265–285, https://doi.org/10.1016/J.ADVMS.2020.04.001.
[7] J. Lee, J. Hyun, J. Lee, et al., So you want to image myelin using MRI: an overview and practical guide for myelin water imaging, J. Magn. Reson. Imaging 53 (2) (2021) 360–373, https://doi.org/10.1002/jmri.27059.
[8] J. How, M. Blattner, S. Fowler, A. Wang-Gillam, S.E. Schindler, Chemotherapy-associated posterior reversible encephalopathy syndrome: a case report and review of the literature, Neurologist 21 (6) (2016) 112–117, https://doi.org/10.1097/NRL.0000000000000105.
[9] G. Schroyen, M. Meylaers, S. Deprez, et al., Prevalence of leukoencephalopathy and its potential cognitive sequelae in cancer patients, J. Chemother. 32 (7) (2020) 327–343, https://doi.org/10.1080/1120009X.2020.
[10] J. Petr, L. Hogeboom, P. Nikulin, et al., A systematic review on the use of quantitative imaging to detect cancer therapy adverse effects in normal-appearing brain tissue, Magn. Reson. Mater. Phys., Biol. Med. (2021) 1–24, https://doi.org/10.1007/S10334-021-00985-2. *2021*December.
[11] M.B. De Ruiter, L. Reneman, W. Boogerd, et al., Late effects of high-dose adjuvant chemotherapy on white and gray matter in breast cancer survivors: converging results from multimodal magnetic resonance imaging, Hum. Brain Mapp. 33 (12) (2012) 2971–2983, https://doi.org/10.1002/hbm.21422.
[12] G. Schroyen, J. Vissers, A. Smeets, et al., Blood and neuroimaging biomarkers of cognitive sequelae in breast cancer patients throughout chemotherapy: a systematic review, Transl. Oncol. 16 (2022), 101297, https://doi.org/10.1016/J.TRANON.2021.101297.
[13] N.J. Ashton, S. Janelidze, A. Al Khleifat, et al., A multicentre validation study of the diagnostic value of plasma neurofilament light, Nat. Commun. 12 (1) (2021) 3400, https://doi.org/10.1038/s41467-021-23620-z.
[14] G.N. Hortobagyi, S.B. Edge, A. Giuliano, New and important changes in the TNM staging system for breast cancer, Am. Soc. Clin. Oncol. Educ. book Am. Soc. Clin. Oncol. Annu. Meet. 38 (38) (2018) 457–467, https://doi.org/10.1200/EDBK_201313.
[15] S. Jain, D.M. Sima, A. Ribbens, et al., Automatic segmentation and volumetry of multiple sclerosis brain lesions from MR images, Neuroimage (Amst) 8 (2015) 367, https://doi.org/10.1016/J.NICL.2015.05.003.
[16] M. Rakić, S. Vercruyssen, S. Van Eyndhoven, et al., icobrain ms 5.1: combining unsupervised and supervised approaches for improving the detection of multiple sclerosis lesions, NeuroImage Clin. 31 (2021), https://doi.org/10.1016/J.NICL.2021.102707.
[17] A.J. Thompson, B.L. Banwell, F. Barkhof, et al., Diagnosis of multiple sclerosis: 2017 revisions of the McDonald criteria, Lancet Neurol. 17 (2) (2018) 162–173, https://doi.org/10.1016/S1474-4422(17)30470-2.
[18] K. Poesen, M. De Schaepdryver, B. Stubendorff, et al., Neurofilament markers for ALS correlate with extent of upper and lower motor neuron disease, Neurology 88 (24) (2017) 2302–2309, https://doi.org/10.1212/WNL.0000000000004029.
[19] J. Gaiottino, N. Norgren, R. Dobson, et al., Increased neurofilament light chain blood levels in neurodegenerative neurological diseases, PLoS One 8 (9) (2013) 75091, https://doi.org/10.1371/journal.pone.0075091.
[20] M. Koller, robustlmm: An R package for robust estimation of linear mixed-effects models, J. Stat. Softw. 75 (6) (2016) 1–24, https://doi.org/10.18637/jss.v075.i06.
[21] J.L. Bernal-Rusiel, D.N. Greve, M. Reuter, B. Fischl, M.R. Sabuncu, Statistical analysis of longitudinal neuroimage data with Linear Mixed Effects models, Neuroimage 66 (2013) 249–260, https://doi.org/10.1016/j.neuroimage.2012.10.065.
[22] S.M. Choi, S.H. Lee, Y.S. Yang, B.C. Kim, M.K. Kim, K.H. Cho, 5-fluorouracil-induced leukoencephalopathy in patients with breast cancer, J. Korean Med. Sci. 16 (3) (2001) 328–334, https://doi.org/10.3346/jkms.2001.16.3.328.
[23] C.A. Moore-Maxwell, M.B. Datto, C.M. Hulette, Chemotherapy-induced toxic leukoencephalopathy causes a wide range of symptoms: a series of four autopsies, Mod. Pathol. (2004), https://doi.org/10.1038/modpathol.3800049.
[24] R.J. Ferguson, B.C. McDonald, A.J. Saykin, T.A. Ahles, Brain structure and function differences in monozygotic twins: possible effects of breast cancer chemotherapy, J. Clin. Oncol. 25 (25) (2007) 3866–3870, https://doi.org/10.1200/JCO.2007.10.8639.
[25] G. Schroyen, C. Sleurs, E. Bartsoen, et al., Neuroinflammation as potential precursor of leukoencephalopathy in early-stage breast cancer patients: a cross-sectional PET-MRI study, Breast 62 (2022) 61–68, https://doi.org/10.1016/J.BREAST.2022.02.001.
[26] S. Menning, M.B. De Ruiter, D.J. Veltman, et al., Changes in brain white matter integrity after systemic treatment for breast cancer: a prospective longitudinal study, Brain Imaging Behav. 12 (2) (2017) 324–334, https://doi.org/10.1007/s11682-017-9695-x.
[27] V. Koppelmans, M.W. Vernooij, W. Boogerd, et al., Prevalence of cerebral small-vessel disease in long-term breast cancer survivors exposed to both adjuvant radiotherapy and chemotherapy, J. Clin. Oncol. 33 (6) (2015) 588–593, https://doi.org/10.1200/JCO.2014.56.8345.
[28] E.M. Gibson, S. Nagaraja, A. Ocampo, et al., Methotrexate chemotherapy induces persistent tri-glial dysregulation that underlies chemotherapy-related cognitive impairment, Cell 176 (1–2) (2019) 43–55, https://doi.org/10.1016/J.CELL.2018.10.049, e13.
[29] E.M. Gibson, M. Monje, Microglia in cancer therapy-related cognitive impairment, Trend. Neurosci. 44 (6) (2021) 441–451, https://doi.org/10.1016/J.TINS.2021.02.003.

[30] D. Fuhrmann, D. Nesbitt, M. Shafto, et al., Strong and specific associations between cardiovascular risk factors and white matter micro- and macrostructure in healthy aging, Neurobiol. Aging 74 (2019) 46–55, https://doi.org/10.1016/J.NEUROBIOLAGING.2018.10.005.
[31] L. Griffanti, M. Jenkinson, S. Suri, et al., Classification and characterization of periventricular and deep white matter hyperintensities on MRI: a study in older adults, Neuroimage 170 (2018) 174–181, https://doi.org/10.1016/J.NEUROIMAGE.2017.03.024.
[32] G. Schroyen, J. Blommaert, D. van Weehaeghe, et al., Neuroinflammation and its association with cognition, neuronal markers and peripheral inflammation after chemotherapy for breast cancer, Cancers (Basel) 13 (16) (2021).
[33] K. Akgün, N. Kretschmann, R. Haase, et al., Profiling individual clinical responses by high-frequency serum neurofilament assessment in MS, Neurol. Neuroimmunol. neuroinflammat. 6 (3) (2019), https://doi.org/10.1212/NXI.0000000000000555.
[34] A. Natori, T. Ogata, M. Sumitani, T. Kogure, T. Yamauchi, H. Yamauchi, Potential role of pNF-H, a biomarker of axonal damage in the central nervous system, as a predictive marker of chemotherapy-induced cognitive impairment, Clin. Cancer Res. 21 (6) (2015) 1348–1352, https://doi.org/10.1158/1078-0432.CCR-14-2775.
[35] S. Karteri, J. Bruna, A.A. Argyriou, et al., Prospectively assessing serum neurofilament light chain levels as a biomarker of paclitaxel-induced peripheral neurotoxicity in breast cancer patients, J. Peripher. Nerv. Syst. (2022), https://doi.org/10.1111/JNS.12493. April.
[36] A. Frank, J. Bendig, I. Schniewind, et al., Serum neurofilament indicates that DBS surgery can cause neuronal damage whereas stimulation itself does not, Sci. Rep. 12 (1) (2022) 1–5, https://doi.org/10.1038/s41598-022-05117-x. *2022 121*.
[37] C.L. Loprinzi, C. Lacchetti, J. Bleeker, et al., Prevention and management of chemotherapy-induced peripheral neuropathy in survivors of adult cancers: ASCO guideline update, J. Clin. Oncol. 38 (28) (2020) 3325–3348, https://doi.org/10.1200/JCO.20.01399.
[38] S.G. Wu, S.J. Huang, J. Zhou, et al., Dosimetric analysis of the brachial plexus among patients with breast cancer treated with post-mastectomy radiotherapy to the ipsilateral supraclavicular area: report of 3 cases of radiation-induced brachial plexus neuropathy, Radiat. Oncol. 9 (2014) 292, https://doi.org/10.1186/S13014-014-0292-5.
[39] R. Velasco, A.A. Argyriou, C. Marco, et al., Serum neurofilament levels correlate with electrodiagnostic evidence of axonal loss in paclitaxel-induced peripheral neurotoxicity, J. Neurol. 270 (1) (2023) 531–537, https://doi.org/10.1007/S00415-022-11377-4.
[40] Å. Sandelius, H. Zetterberg, K. Blennow, et al., Plasma neurofilament light chain concentration in the inherited peripheral neuropathies, Neurology 90 (6) (2018) e518–e524, https://doi.org/10.1212/WNL.0000000000004932.
[41] J. Louwsma, A.F. Brunger, J. Bijzet, et al., Neurofilament light chain, a biomarker for polyneuropathy in systemic amyloidosis, Amyloid 28 (1) (2021) 50–55, https://doi.org/10.1080/13506129.2020.1815696.
[42] J. Kuhle, H. Kropshofer, D.A. Haering, et al., Blood neurofilament light chain as a biomarker of MS disease activity and treatment response, Neurology 92 (10) (2019) E1007–E1015, https://doi.org/10.1212/WNL.0000000000007032.
[43] M. Li, K. Caeyenberghs, Longitudinal assessment of chemotherapy-induced changes in brain and cognitive functioning: a systematic review, Neurosci. Biobehav. Rev. 92 (2018) 304–317, https://doi.org/10.1016/j.neubiorev.2018.05.019.
[44] A. Amidi, L.M. Wu, Structural brain alterations following adult non-CNS cancers: a systematic review of the neuroimaging literature, Acta Oncol. 58 (5) (2019) 522, https://doi.org/10.1080/0284186X.2018.1563716.
[45] A.R. Gafson, N.R. Barthélemy, P. Bomont, et al., Neurofilaments: neurobiological foundations for biomarker applications, Brain 143 (7) (2020) 1975, https://doi.org/10.1093/BRAIN/AWAA098.
[46] C. Gasperini, L. Prosperini, M. Tintoré, et al., Unraveling treatment response in multiple sclerosis: a clinical and MRI challenge, Neurology 92 (4) (2019) 180–192, https://doi.org/10.1212/WNL.0000000000006810.
[47] A.A. Argyriou, S. Karteri, J. Bruna, et al., Serum neurofilament light chain levels as biomarker of paclitaxel-induced cognitive impairment in patients with breast cancer: a prospective study, Support. Care Cancer 30 (2) (2022) 1807–1814, https://doi.org/10.1007/S00520-021-06509-X.